Anal. Chem. **2006,** *78,* 1913−1920

Gold Nanoparticle-Enhanced Secondary Ion Mass Spectrometry Imaging of Peptides on Self-Assembled Monolayers

Young-Pil Kim,† Eunkeu Oh,† Mi-Young Hong,† Dohoon Lee,† Min-Kyu Han,† Hyun Kyong Shon,‡ Dae Won Moon,‡ Hak-Sung Kim,*,† and Tae Geol Lee*,‡

Department of Biological Sciences, Korea Advanced Institute of Science and Technology, 373-1, Kusung-Dong, Yusung-Gu, Daejeon 305-701, Korea, and Nano-Surface Group, Korea Research Institute of Standards and Science, Daejeon 305-600, Korea

We demonstrate the use of gold nanoparticles (AuNPs) to enhance the secondary ion emission of peptides in time-of-flight secondary ion mass spectrometry (TOF-SIMS). The signal intensity of peptides adsorbed onto AuNPs was significantly increased when compared to that of self-assembled monolayers (SAMs). This gold nanoparticle-enhanced SIMS, termed NE-SIMS, enabled the sensitive detection of subtle modifications of peptides, such as phosphorylation. From a quantitative analysis of the amounts of adsorbed peptides and AuNPs on SAMs using quartz crystal microbalance and surface plasmon resonance spectroscopy, the ratio of peptide molecule to AuNP on amine-SAMs was revealed to be 18−19:1. When considering the ratio of peptide to matrix ($1:10^3-10^6$) employed in a matrix-enhanced SIMS, the use of AuNPs gave rise to a significantly increased secondary ion emission of peptides. Peptides were adsorbed onto patterned AuNPs on SAMs using a microfluidic system, and well-contrasted molecular ion images were obtained. NE-SIMS is expected to be applied to a chip-based analysis of modification of biomolecules in a label-free manner.

The electrospray ionization and matrix-assisted laser desorption/ionization (MALDI) techniques represent significant advancements within many biotechnological fields since the generation of characteristic molecular or quasi-molecular ions from biomolecules is essential for analyzing many biological systems.[1] Extending the scope of these techniques requires novel methods of enhancing ion signals with reliable sample preparations to allow selective identification of complex biomolecules that would otherwise not be easily detected. Recently, size-selected (2−10 nm) gold nanoparticles (AuNPs) were used as a matrix in laser desorption/ionization mass spectrometry, enabling the selective and sensitive detection of phosphopeptides.[2] Yet, although AuNPs are widely used as signal enhancers in various fields,[3] to the best of our knowledge, there are no studies of their collaborative role with time-of-flight secondary ion mass spectrometry (TOF-SIMS) in detecting biomolecules.

Over the past several years, TOF-SIMS has proved to be an effective method for chemically imaging organic/biosurfaces due to its high scan rate and superior spatial resolution.[4] In an effort to expand the use of TOF-SIMS in biotechnological fields, several attempts have been made to increase the emission of the secondary molecular ion of biomolecules,[5] and recent promising approaches involve the incorporation of various signal enhancers with the use of polyatomic ion analysis beams.[6] However, biological applications of TOF-SIMS analysis still remain a challenge particularly on a biochip surface, since signal enhancers (e.g., matrix) cannot be homogeneously and selectively deposited onto the chip surface and cannot be effectively bound with biomolecules immobilized on nonmetallic surfaces, such as the self-assembled monolayers (SAMs). To expand the potential of TOF-SIMS imaging in a chip-based analysis of biomolecues requires a strategy to induce an efficient molecular ion emission of biomolecules and to ensure a homogeneous distribution of signal

* To whom correspondence should be addressed. E-mail: hskim76@kaist.ac.kr. Tel: +82-42-869-2616. Fax: +82-42-869-2610. E-mail: tglee@kriss.re.kr. Tel: +82-42-868-5129. Fax: +82-42-868-5032.

† Korea Advanced Institute of Science and Technology.

‡ Korea Research Institute of Standards and Science.

(1) (a) Aebersold, R.; Mann, M. *Nat. Insight* **2003**, *422*, 198−207. (b) Stutz H. *Electrophoresis* **2005**, *26*, 1254−1290. (c) Houseman, B. T.; Huh, J. H.; Kron, S. J.; Mrksich, M. *Nat. Biotechnol.* **2002**, *20*, 270−274.

(2) McLean, J. A.; Stumpo, K. A.; Russell, D. H. *J. Am. Chem. Soc.* **2005**, *127*, 5304−5305.

(3) (a) Daniel, M.-C.; Astruc, D. *Chem. Rev.* **2004**, *104*, 293−346. (b) He, T.; Ma, Y.; Cao, Y.; Jiang, P.; Zhang, X.; Yang, W.; Yao, J. *Langmuir* **2001**, *17*, 8024−8027. (c) Wang, Z.; Lee, J.; Cossins, A. R.; Brust, M. *Anal. Chem.* **2005**, *77*, 5770−5774. (d) Natan, M. J.; Lyon, L. A. In *Metal Nanoparticless Synthesis, Characterization and Applications*; Feldheim, D. L., Colby, A. F., Jr., Eds.; Marcel Dekker: New York, 2002; pp 183−205. (e) Félidj, N.; Aubard, J.; Lévi, G.; Krenn, J. R.; Hohenau, A.; Schider, G.; Leitner, A.; Aussenegg, F. R. *Appl. Phys. Lett.* **2003**, *82*, 3095−3097.

(4) (a) Altelaar, A. F. M.; van Minnen, J.; Jiménez, C. R.; Heeren, R. M. A.; Piersma, S. R. *Anal. Chem.* **2005**, *77*, 735−741. (b) Braun, R. M.; Beyder, A.; Xu, J. Y.; Wood, M. C.; Ewing, A. G.; Winograd, N. *Anal. Chem.* **1999**, *71*, 3318−3324. (c) Pacholski, M. L.; Winograd, N. *Chem. Rev.* **1999**, *99*, 2977−3005. (d) Ostrowski, S. G.; Van Bell, C. T.; Winograd, N.; Ewing, A. G. *Science* **2004**, *305*, 71−73.

(5) (a) Winograd, N. *Anal. Chem.* **2005**, *77*, 142A−149A. (b) Handley, J. *Anal. Chem.* **2002**, *74*, 335A−341A.

(6) (a) Xua, J.; Ostrowskia, S.; Szakala, C.; Ewingb, A. G.; Winograd, N. *Appl. Surf. Sci.* **2004**, *231−232*, 159−163. (b) Wu, K. J.; Odom. R. W. *Anal. Chem.* **1996**, *68,* 873−882. (c) Michel, R.; Luginbuhl, R.; Graham, D. J.; Ratner, B. D. *J. Vac. Sci. Technol. A* **2000**, *18*, 1114−1118. (d) McArthur, S. L.; Vendettuoli, M. C.; Ratner, B. D.; Castner, D. G, *Langmuir* **2004**, *20*, 3704−3709. (e) Delcorte, A.; Medard, N.; Bertrand, P. *Anal. Chem.* **2002**, *74*, 4955−4968; *Anal. Chem.* **2005**, *77*, 2107−2115.

10.1021/ac051500j CCC: $33.50
Published on Web 02/07/2006

enhancers with sensitivity and selectivity on a well-controlled surface such as SAMs.

In this paper, we demonstrate the effect of AuNPs on secondary ion emission of peptides in TOF-SIMS. Our approach, designated gold nanoparticle-enhanced (NE)-SIMS, involved TOF-SIMS imaging of peptides adsorbed onto a SAM/AuNPs assembly and resulted in a significant increase of secondary ion emission of peptides when compared to that of SAMs. As a target analyte, a peptide and its phosphopeptide were used as proof of concept for our application of the SAM/AuNPs system in analyzing the posttranslational modifications because the enhanced ion signals from the peptides on SAM/AuNPs would permit both a sufficient mass range (<1000 Da) and a sensitive mass detection of subtle modification within the peptide sequence in TOF-SIMS. Peptides were adsorbed onto patterned AuNPs on SAMs using a microfluidic system, and well-contrasted molecular ion images were obtained.

EXPERIMENTAL SECTION

Materials. Hydrogen tetrachloroaurate(III) trihydrate (99.9% $HAuCl_4 \cdot 3H_2O$), sodium citrate dihydrate (trisodium salt, $C_6H_5Na_3O_7 \cdot 2H_2O$), and sodium borohydride (99%) were purchased from Sigma-Aldrich. The reagents used in the preparation of SAMs were all purchased from commercial sources: 99% 11-mecaptoundecanoic acid (MUA, Aldrich); 99% 3-mercaptopropionic acid (MPA, Aldrich); 90% 6-mercaptonicotinic acid (MNA, Aldrich); 99% 11-mercaptoundecylamine (MUAM, Dojindo); and 99% (3-aminopropyl)triethoxysilane (APTES, Aldrich). Peptides (P1, Ac-PRNYVTP-NH_2; P2, Ac-PRNYpVTP-NH_2) were all synthesized by Peptron, Inc..

Formation of SAMs. A gold substrate was prepared by sequentially evaporating a 400-Å-thick film of Ti and a 1500-Å-thick film of gold onto a Si wafer. Prior to the monolayer deposition, the substrates (Au, Si) were cut into 10 mm × 10 mm sections and cleaned for 5 min by immersion in a piranha solution (1:4) 30% H_2O_2/concentrated H_2SO_4 (v/v). *Caution*: the piranha solution reacts violently with most organic materials and must be handled with extreme care. The substrates were then washed sequentially with distilled water and absolute ethanol. A mica gold (111) substrate (1.4 cm × 1.1 cm, Molecule Imaging Inc.), surface plasmon resonance (SPR) gold sensor chip (SIA kit Au, BIAcore), and QCM gold crystal (Sensor Crystal QSX 301) were also prepared to construct the SAMs and used in the analyses. Prior to the SAM formation, the mica gold substrate (1500-Å-thick gold film) was annealed and cleaned with a hydrogen flame. The SPR and QCM gold sensor chips were cleaned with 0.1 N NaOH containing 1% Triton-X for 5 min, followed by a thorough rinsing with water, and additionally treated with an oxygen−plasma cleaner for 2 min prior to use. For the formation of carboxy SAMs, various gold substrates were immersed overnight in a 2 mM solution of one of the self-assembly reagents (MUA, MPA, MNA) in absolute ethanol. To attach the AuNPs onto the surfaces, the formation of amine SAMs was first induced onto each substrate by immersing each chip in a 2 mM solution of MUAM in absolute ethanol for 2 h. Mica gold, SPR gold sensor chip, and QCM gold crystal were also derivatized with MUAM SAMs using the same procedure. A silicon substrate was derivatized with a 10% methanol solution of APTES for 2 h, followed by a thorough rinsing with methanol for the TOF-SIMS analysis. An amine-functionalized glass substrate was prepared by using a plasma-polymerized ethylenediamine (PPEDA) film method,[7] where ethylenediamine monolayers were deposited by applying 3 W of inductively coupled plasma power.

Synthesis of Gold Nanoparticles. AuNPs were synthesized by reduction and stabilization with citrate as described elsewhere.[8] Briefly, 0.1 g of $HAuCl_4 \cdot 3H_2O$ (0.1% (w/w), Aldrich) was dissolved in 100 mL of distilled water and vigorously stirred for 1 min. To this solution, 0.02 g of sodium citrate dihydrate (2-hydroxy-1,2,3-propanetricarboxylic acid) was added, and again the solution was stirred. After 1 min, for the reduction and formation of gold colloids, 85 μL of a stock solution containing 11.4 mg of $NaBH_4$ in 1 mL of distilled water was quickly added to the reaction solution, followed by stirring for 5 min. The completely reduced solution containing 254 μM Au was stored at 4 °C. The clustering of AuNPs was estimated by UV−visible spectroscopy (UV-2550, Shimadzu), and the size of AuNPs was confirmed to be 3.2 nm (±0.4 nm SD, $n = 100$) using energy-filtering transmission electron microscopy (EF-TEM, EM912 Omega, Carl Zeiss). Monolayers of AuNPs were formed by a 30-min deposition of AuNPs on the amine-functionalized Si, Au, or glass surface, followed by washing with distilled water. The peptides, dissolved in water, were directly adsorbed onto bare gold or Au/carboxy SAMs (MUA, MPA, MNA) or AuNPs assembly for 60 min with the same concentration of solution (50 $\mu g \cdot mL^{-1}$), and the surfaces were sequentially washed with distilled water and dried under a stream of N_2. The optimal concentration of peptide for the reaction was determined by the SIMS intensity at m/z $[P1 + H]^+$ as a function of solution concentration of peptide P1 (Figure S1, Supporting Information).

Atomic Force Microscopy (AFM) Imaging. Tapping-mode AFM imaging was performed with a Dimension-3100 AFM (Veeco Digital Instruments) equipped with a Nanoscope IIIa controller. Supersharp tips (SSS NCH-10, Nanoworld AG) with a nominal tip radius of less than 5 nm at resonance frequencies of 240−270 kHz were used in all image collections. All measurements were carried out at ambient temperature in air with 512 × 512 data acquisitions at a scan size of 1 × 1 μm^2. Scan rate, set point, and proportional gain values were adjusted according to each sample condition during the scanning process. Grain analysis and surface roughness of the scanned images were determined after first-order flattening using the Nanoscope IIIa software (version 5.30r2).

Quartz Crystal Microbalance (QCM) Analysis. To quantify surface-attached AuNPs, a QCM measurement was performed using a Q-Sense D300 system (Q-Sense AB). A gold-coated AT-cut quartz crystal was used to monitor the amount of AuNPs. Gold crystal was cleaned and modified with MUAM SAMs according to the above procedure. The amine-modified crystal was finally washed with ethanol and distilled water and then dried under a flow of nitrogen prior to use. For measurements, the crystal was mounted in a thermal static liquid chamber, and the stable baseline on the surface was then confirmed during the prewashing step with distilled water. Adsorption of gold nanoparticles was conducted by passing a 1-mL solution of AuNPs over the surface at

(7) Kim, J.; Shon, H. K.; Jung, D.; Moon, D. W.; Han, S. Y.; Lee, T. G.. *Anal. Chem.* **2005**, *77*, 4137−4141.

(8) (a) Frens, G. *Nat. Phys. Sci.* **1973**, *241*, 20−22. (b) Handley, D. E. In *Colloidal Gold: Principles, Methods, and Applications*; Hayat, M. A., Ed.; Academic Press: New York, 1989; Vol 1, Chapter 2, pp 13−32.

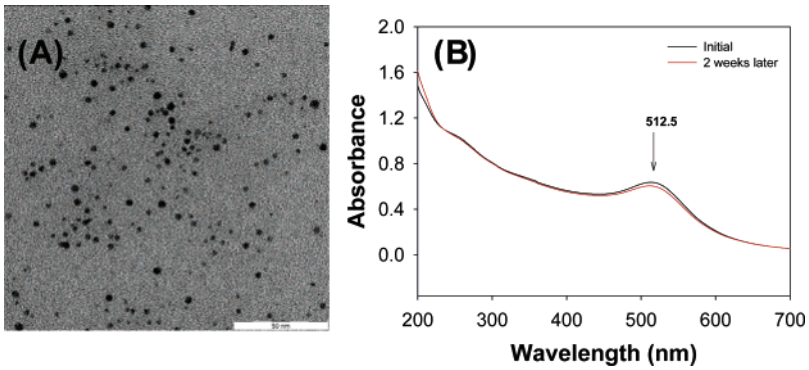

Figure 1. (A) Energy-filtering TEM image and (B) UV−visible spectrum of citrate-stabilized AuNPs. Mean diameter of AuNPs is 3.2 nm (SD ±0.4, $n = 100$). The UV spectrum of AuNPs in solution was stable for 2 weeks.

Chart 1. Schematic Representation of AuNP-Enhanced SIMS Analysis of Peptides[a]

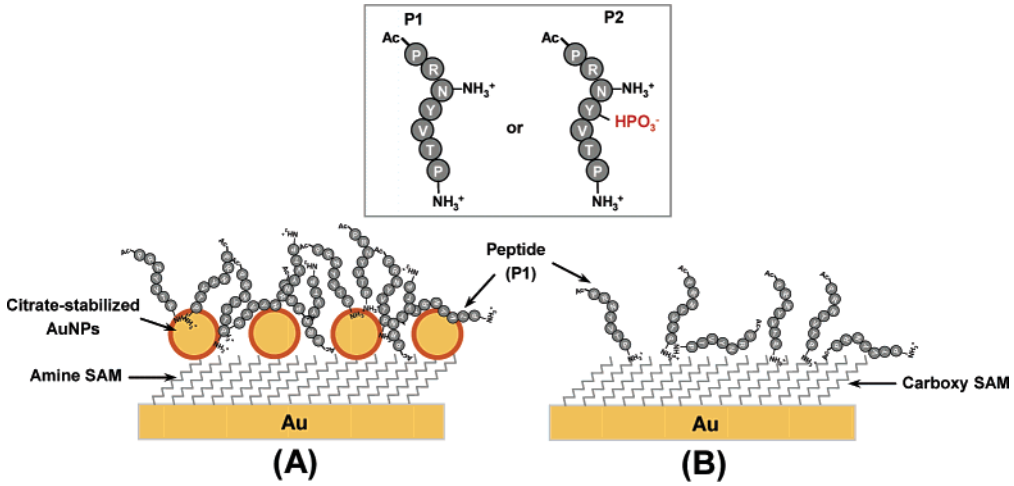

[a] AuNPs were electrostatically attached to (A) amine-terminated SAMs. As a control, peptides were directly adsorbed onto (B) carboxy-terminated SAMs

room temperature and then sequentially returned to distilled water for 5 min. Time-course changes in the resonant frequency (Δf) and energy dissipation (ΔD) were measured simultaneously at the fundamental resonant frequency (5 MHz).

Microfluidic Patterning and SPR Spectroscopy. Microfluidic patterning and SPR analysis were performed with a BIAcore-X instrument (BIAcore) on gold sensor chips. Each flow channel with a 500-μm width was used to generate uniformly patterned lines by exposing the surface to different analytes. A gold sensor chip modified with MUAM SAMs was attached to a chip socket, docked to a SPR instrument, and then washed with distilled water for cleaning. For a different line patterning of AuNPs/peptides (P1 and P2), the electrostatic adsorption of anionic AuNPs at both of two channels was first carried out by passing a 254 μM solution in water for 30 min over the cationic surface at a flow rate of 3 μL·min^{-1} at 25 °C and then sequentially returned to distilled water. After the attachment of AuNPs, two peptides were separately injected through the two microfluidic channels over the AuNP surface for 30 min (P1, 50 μg·mL^{-1} in flow channel 1; P2, 50 μg·mL^{-1} in flow channel 2). After washing with distilled water, a relative shift in the BIAcore response unit (RU) for the adsorption of AuNPs and peptides was monitored for quantitative analysis. As a control experiment, a bare gold chip, a carboxy-modified gold chip, and an amine-modified gold chip were used for the direct adsorption of the P1 and P2 peptides (P1, channel 1; P2, channel 2) without AuNPs being attached. The amount of peptides over each surface was then determined after 30 min and compared with those on AuNPs.

TOF-SIMS Analysis. TOF-SIMS was carried out using a TOF-SIMS V instrument (ION-TOF GmbH) with 25-keV Au_1^+ primary ions (average current of 0.8 pA, pulse width of 16.8 ns, repetition rate of 5 kHz). The analysis area of 500 × 500 μm^2 was randomly rastered by primary ions for spectrum analysis. The primary ion dose was maintained below 10^{13} ions·cm^{-2} to ensure static SIMS condition. Mass resolution was usually higher than 5000 at m/z 197 in the positive mode. Positive ion spectra were internally calibrated using H^+, H_2^+, CH_3^+, $C_2H_3^+$, and $C_3H_4^+$ peaks. TOF-SIMS images for patterned peptides were obtained by rastering the 25-keV Au_1^+ beam over a surface area of 300 × 300 μm^2 with a primary ion influence of 4 × 10^{12} ions·cm^{-2}.

RESULTS AND DISCUSSION

Synthesis and Layers of AuNPs. The TEM image and absorption spectrum confirmed that the prepared AuNPs were spherical with an average diameter of 3.2 nm and that the characteristic SPR band was observed at ~512 nm (Figure 1). The citrate-stabilized nanoparticle suspension was stable for at least 2 weeks at 4 °C (Figure 1B). To facilitate the assembly of a more stable AuNP layer, amine-ended SAMs were employed because amine-functionalized surfaces are capable of binding

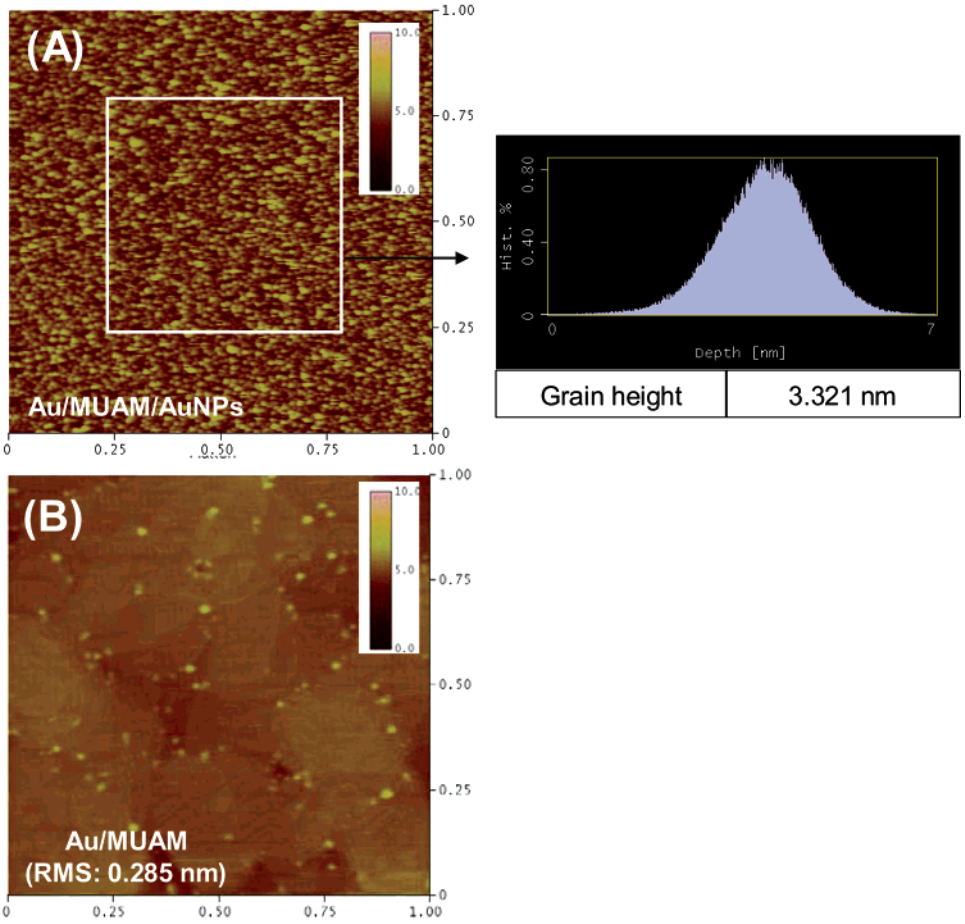

Figure 2. Surface AFM images of (A) Au/MUAM/AuNPs and (B) Au/MUAM. In the inset area (white box), grain analysis showed protruding spots of AuNPs that were distinguished with heights of 3.3 nm.

colloidal particles through electrostatic interactions between the positive amine terminus (cationic SAMs) and negative AuNPs (Chart 1A).[9] The formation of the AuNP monolayer was thus achieved by placing the gold substrate modified with SAMs of MUAM in a solution of AuNPs. Topographic information of the monolayer was obtained from AFM images as shown in Figure 2. Compared with MUAM SAMs on mica gold in which the roughness was less than 0.3 nm (Figure 2B), the AuNP-attached surface showed a distinct vertical fluctuation of the nanoparticles that were homogeneously arranged on the gold surface (Figure 2A). From grain analysis in the inset area, the height (depth) of the molecules was determined to be within 3.3 nm to the background surface, similar to the size of the spherical AuNPs revealed by a TEM image (Figure 1A). The surface coverage of AuNPs from the AFM image was estimated to be $\sim 5.0 \times 10^{11}$ particles·cm^{-2}, which could be an underestimation due to tip−sample convolution. For a clearer quantification of AuNPs, the surface density (number of particles·cm^{-2}) of the AuNP monolayer was determined using a quartz crystal microbalance including a dissipation factor measurement (QCM-D).

In Figure 3, the amount of AuNPs adsorbed onto a MUAM-modified gold crystal was quantified by the frequency shift (Δf, black line) of −34.5 Hz, which can be easily converted to a gain

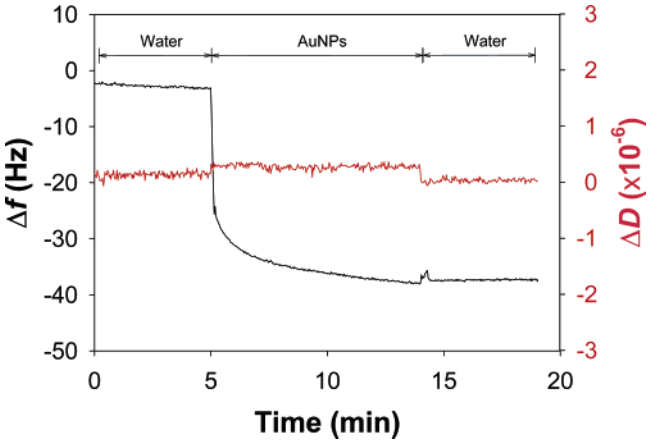

Figure 3. QCM response of AuNPs and peptides sequentially adsorbed on to amine-terminated MUAM SAMs on a gold sensor. Changes in frequency (black line) and dissipation (red line) were simultaneously traced in a 5-MHz crystal.

in mass of 611 ng·cm^{-2}.[10] In contrast to the abrupt decrease in frequency, the dissipation energy (ΔD, red line) with viscoelastic properties showed a relatively small shift of 0.3×10^{-6}, indicating the formation of a rigid layer of AuNPs. The mass change was calculated to be a surface density of $\sim 1.9 \times 10^{12}$ nanoparticles·cm^{-2},

(9) (a) Schmitt, J.; Mächtle, P.; Eck, D.; Möhwald, H.; HelmLa, C. A. *Langmuir* **1999**, *15*, 3256−3266. (b) Grabar, K. C.; Freeman, R. G.; Hommer, M. B.; Natan, M. J. *Anal. Chem.* **1995**, *67*, 735−743.

(10) According to the Q-sense AB, sensitivity constant (C) of QCM-D crystal is 17.7 ng·cm^{-2}·Hz^{-1} at a fundamental frequency ($f_0 \approx 5$ MHz).

Table 1. Surface Density of AuNPs Measured with QCM Crystal

analyte	frequency change (Δf)	mass change[b] ($ng \cdot cm^{-2}$)	surface density[c] (10^{-12} $mol \cdot cm^{-2}$)	surface fractional coverage[d] (%)	relative surface area (%)[e]
AuNPs[a]	34.5 Hz	611.4	3.1	16.5	29.7

[a] AuNPs were estimated to possess 1012 atoms within a mean diameter of 3.2 nm, according to previous literature.[19] [b] A 1-Hz change in QCM-D corresponded to a mass change of 17.7 $ng \cdot cm^{-2}$. [c] Molecular mass of AuNPs is 1.99×10^5 $g \cdot mol^{-1}$. [d] Surface fractional coverage is a relative percentage divided by the 2D hexagonal packing density.[20] [e] Surface area is a relative percentage divided by the flat surface area (1×1 cm^2). This value was determined by multiplying half of spherical surface area of one gold particle ($^1/_2 4\pi R^2$, $R = 1.6$ nm) by the number of particles ($/cm^2$), considering the available area exposed on the surface.

which corresponds to the submonolayer coverage (~17%). This surface fractional coverage is a relative percentage divided by the 2D hexagonal packing density of the nanoparticles on the surface (Table 1). It should be noted that the fractional coverage of citrate-stabilized AuNPs on the amine-modified surface is considerably smaller than the saturation coverage by the 2D random sequential adsorption of hard spheres.[11] Low surface coverage indicates that well-spaced submonolayers of AuNPs were present on the surface due to electrostatic repulsion between the negatively charged nanoparticles (Figure 2A).

NE-SIMS Analysis of Peptides. As typical analytes for NE-SIMS analysis, a peptide (P1, Ac-PRNYVTP-NH_2, MW 886.47) and its phosphorylated form (P2, Ac-PRNYpVTP-NH_2, MW 966.47) were used since they not only have a low mass range to be resolved by SIMS but can provide stability for their biological activities on a chip surface.[12] This short peptide is a portion of the SH3 (Src homology 3) domain within the Grb2 (growth factor receptor binding protein-2), which serves as a target substrate for Abl kinase.[13] The subsequent adsorption of peptides on the layer of AuNPs can be conducted at high spatial densities because the α-amino group at the amidated C-terminus and the guanidinyl group of arginine of the P1 and P2 peptides were presumed to preferentially adhere to the anionic AuNPs as depicted in Chart 1A. As a control, the signals from peptides adsorbed on anionic SAMs were compared to those on anionic AuNPs. Therefore, the direct adsorption of peptide P1 was examined on the carboxy-terminated SAMs with MUA on a gold surface (Chart 1B). To get some insight into the effect of underlying SAMs on the emission of peptides, MNA SAMs with an aromatic ring structure and amine-functionalized SAMs (MUAM) were also included in the measurement. As a result, relatively strong signals of molecular ions (P1, $[P1 + H]^+$ at m/z 887; P2, $[P2 + H]^+$ at m/z 967) were detected on MUAM/AuNPs (Figure 4, D1 and D2). On the other hand, TOF-SIMS analyses of peptide P1 and P2 directly adsorbed onto two carboxy (MUA and MNA) and amine SAMs (MUAM) resulted in very weak corresponding peaks (Figure 4, A1 and A2 for MUA, B1 and B2 for MNA, and C1 and C2 for MUAM).

The thickness of SAMs used did not critically affect the signal intensity of the peptides. When two carboxy SAMs of different thicknesses were examined (11-MUA and 3-MPA SAMs), the

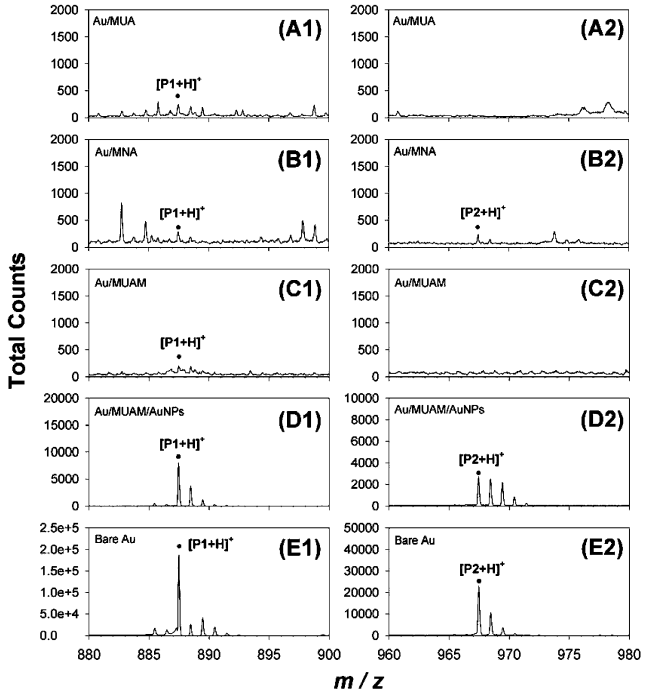

Figure 4. Positive SIMS spectra of peptides (P1, Ac-PRNYVTP-NH_2; P2, Ac-PRNYpVTP-NH_2) on surfaces: (A1, A2) Au/MUA, (B1, B2) Au/MNA, (C1, C2) Au/MUAM, (D1, D2) Au/MUAM/AuNPs, and (E1, E2) bare Au. Left and right panels show SIMS spectra of P1 (MW = 886.47) and P2 (MW = 966.47), respectively. TOF-SIMS analysis was conducted using a Au_1^+ primary ion gun with ion dose below 10^{13} ions$\cdot cm^{-2}$ at a sample area of 500×500 μm^2.

difference in peptide intensity (P1) was much less than the difference by the gold-enhanced signal intensity, although the MPA SAMs showed a slightly higher intensity than the MUA SAMs (Figure S2, Supporting Information). Compared to matrix SAMs such as MNA SAMs, which are known to be effective ion enhancers,[6c,d] the NE-SIMS showed a higher secondary ion emission for peptide P1 and P2 by 1 order of magnitude (Figure 4, B1 and D1, B2 and D2). This observation confirms that AuNPs greatly enhance the emission of secondary molecular ion of peptides. On bare gold, however, secondary ion emission (Figure 4, E1 and E2) was much higher than that for Au/MUAM/AuNPs (Figure 4, D1 and D2). This discrepancy may be due to the differing total surface areas between bare gold and gold nanoparticles. Assuming that synthesized nanoparticles are highly uniform with an average diameter of 3.2 nm (±0.4 nm), two and three-dimensional areas of AuNPs correspond to 16.5 and 29.7% of a flat gold surface, respectively (Table 1). Thus, a bare gold film (1500 Å in thickness) with some slight roughness (1.040 nm

(11) (a) Jin, X.; Wang, N. H. L.; Tarjus, G.; Talbot, J. *J. Phys. Chem.* **1993**, *97*, 4256−4258. (b) Schaaf, P.; Voegel, J.-C.; Senger, B. *J. Phys. Chem.* **2000**, *104*, 2204−2214. (c) Nath, N.; Chilkoti, A. *Anal. Chem.* **2004**, *76*, 5370−5378.

(12) Falsey, J. R.; Renil, M.; Park, S.; Li, S. J.; Lam, K. S. *Bioconjugate Chem.* **2001**, *12*, 346−353.

(13) Li, S.; Couvillon, A. D.; Brasher, B. B.; Van Etten, R. A. *EMBO J.* **2001**, *20*, 6793−6804.

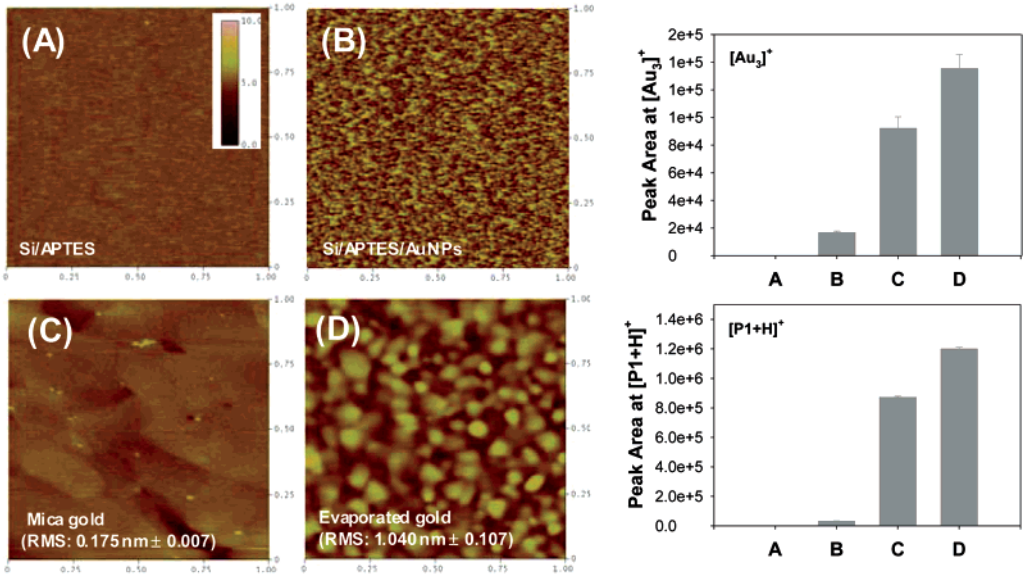

Figure 5. Comparison of ion peak areas ($[Au_3]^+$ and $[P1 + H]^+$) on various surfaces. (A) Si/APTES; (B) Si/APTES/AuNPs; (C) mica gold; (D) evaporated gold substrate. The peptide signal was measured after a 60-min period of adsorption onto different surfaces.

in RMS) would contribute more to the Au-enhanced peptide signal than AuNPs, due to the increased gold surface area. It was also shown that the SIMS intensity of the gold cluster ion (m/z 590.9, Au_3^+) increased as the surface area of the gold increased when it was emitted from the surface by a primary ion (herein referred to as an atomic Au_1 source) impact (Figure 5). A rough gold substrate (Figure 5D) showed a relatively higher generation of gold ions compared to that of AuNPs on an amine-modified Si surface (Figure 5B) or mica gold (Figure 5C), whereas no gold ion signals were detected from the amine-modified Si surface (Figure 5A). The absence of a gold ion signal from the amine-modified Si surface indicates that no implantation of primary gold ion onto the sample surface occurred, due to the static SIMS condition (Figure 5, upper graph). Similar to the generation of gold ions, the generation of P1 peptide ions from each surface also increased as the surface area of the gold increased, although the densities of adsorbed peptides could be different for each surface (Figure 5, lower graph).

To confirm that enhanced ion emission of peptides was mainly attributed to the surface area of gold rather than to the amount of adsorbed peptides, the amount of adsorbed peptides on gold surfaces was determined by using SPR spectroscopy. As shown in Figure 6, the maximum surface densities of P1 (A) and P2 (B) peptides were significantly different, which could be the result of different long-range forces by the differing charge states of the two peptides.[14] Most importantly, the adsorption of peptides onto AuNPs resulted in the maximum surface density of peptides 2−3-fold higher than that on SAMs (Table 2), implying that enhanced ion emission of peptides on AuNPs was caused by the higher density of peptides, as shown in Figure 4, D1/D2. However, signal enhancement was not always linear with increasing peptide density. For example, the MUAM SAMs did not show a significant enhancement of peptide intensity (Figure 4, C1/C2), despite the relatively high density of peptides, compared to the MUA SAMs (Figure 6A, B). Accordingly, it is reasonable that the higher

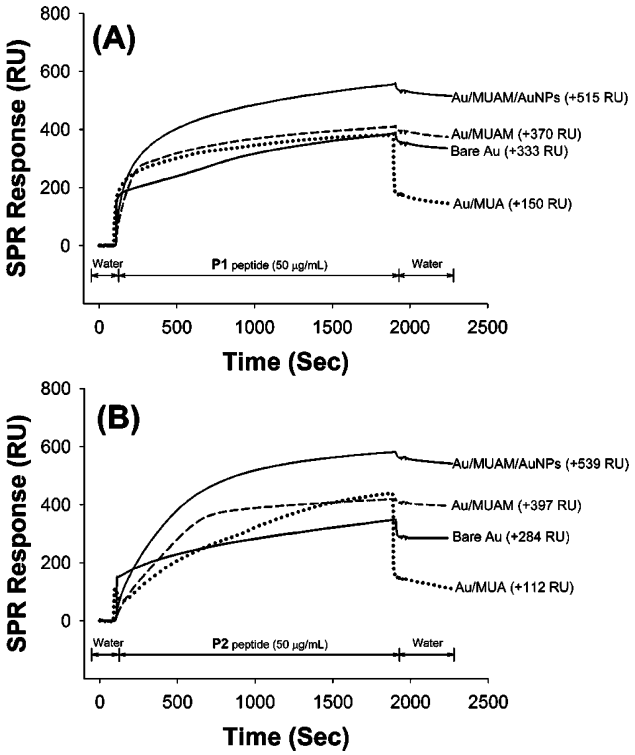

Figure 6. Real-time SPR responses of two peptides (P1 and P2) attached to bare Au, Au/MUA, Au/MUAM, and Au/MUAM/AuNPs. (A) P1 and (B) P2 peptides with a solution of 50 $\mu g \cdot mL^{-1}$ in distilled water were independently loaded in flow channel 1 and flow channel 2, respectively.

peptide intensity on the AuNP assembly, in comparison with SAMs, can be mainly attributed to signal enhancement by the gold nanoparticles. This was supported by the result that the signal enhancement for peptide P1 using AuNPs was much higher than that in the absence of AuNPs (Figure 4, D1/D2 and A1/A2). We believe that the effects of AuNPs on enhancing the secondary ion emission of peptides may be similar to the mechanism observed

(14) (a) Castelino, K.; Kannan, B.; Majumdar, A. *Langmuir* **2005**, *21*, 1956−1961. (b) Clare, B. H.; Abbott, N. L. *Langmuir* **2005**, *21*, 6451−6461.

Table 2. Surface Densities of Peptides Measured by Using SPR

analyte[a]	surface	SPR response change (ΔRU)	surface density		
			ng·cm^{-2}	10^{-12} mol·cm^{-2}	molecules·cm^{-2}
P1	Au/MUA	150	15.0	16.9	1.0×10^{13}
	Au/MUAM	370	37.0	41.7	2.5×10^{13}
	Au/MUAM/AuNPs	515	51.5	58.1	3.5×10^{13}
	bare Au	333	33.3	37.6	2.3×10^{13}
P2	Au/MUA	112	11.2	12.6	8.0×10^{12}
	Au/MUAM	397	39.7	44.8	2.7×10^{13}
	Au/MUAM/AuNPs	539	53.9	60.8	3.7×10^{13}
	bare Au	284	28.4	32.0	1.9×10^{13}

[a] P1, Ac-PRNYVTP-NH_2 (MW = 886.47); P2, Ac-PRNYpVTP-NH_2 (MW = 966.47).

for peptides on a bare gold surface, i.e., protonation due to a reaction between a neutral peptide and a proton during high-energy events, followed by collision cascades.[15] Although the amount of peptide adsorbed on bare gold was relatively low compared to the MUAM/AuNPs assembly, the high areas of gold can trigger enhanced peptide ion generation, as shown in Figure 5. Despite the low ion emission compared to a bare gold surface, however, the use of AuNPs provides an effective gold surface on various substrates for efficient emission of the secondary ions.

In contrast to the analyte/matrix ratio ($1{:}10^3-10^6$) in a matrix-enhanced SIMS,[6b] the ratio of the total number of peptide molecule to AuNP on the amine-modified surface was estimated to be 18:1−19:1 from QCM and SPR data (Tables 1 and 2). From the comparison of the ratios, it is likely that AuNPs would allow a more efficient ion generation, compared to matrixes used in ME-SIMS techniques. This enhancing performance of gold nanoparticles has been demonstrated in MALDI-MS.[2] In addition, the increased concentration of peptides on the AuNP assembly induced an increase in SIMS intensity (Figure S1, Supporting Information); thus, the NE-SIMS can be an effective method of enhancing the secondary ion emission of peptides without secondary ion attenuation from the saturated peptide density.

In addition to signal enhancement, the NE-SIMS technique provides the following advantages. First, the use of AuNPs reduces steric hindrance for the subsequent binding molecules, enabling the effective binding of peptides and allowing kinase access for enzymatic modification, due to the spherical shape of nanoparticles. In our previous work,[16] we found that the layers of spherically shaped dendrimers lead to highly efficient protein−ligand interactions, due to the fact that the lateral steric effect in protein binding is considerably minimized on the dendrimer layers. Similarily, our preliminary study showed that the AuNPs/SAMs assembly resulted in a relatively strong response to the Abl kinase reaction compared to bare gold (Figure S3, Supporting Information). Thus, an application of the SAMs/AuNPs system for analysis of the posttranslational modifications is expected to reveal distinct advantages of the SAMs/AuNPs system. Second, in our SAMs/AuNPs system, it is easy to modify the surface for effectively reducing nonspecific protein binding. This is important because severe nonspecific binding of proteins may cause serious

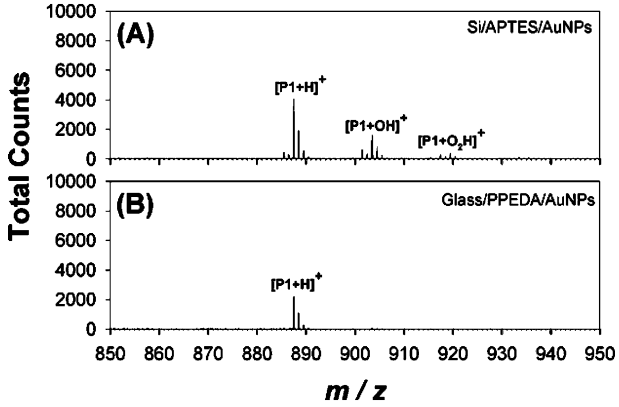

Figure 7. Positive ion gold NE-SIMS spectra of peptide P1 on (A) an APTES-modified silicon surface and (B) a PPEDA-modified glass surface.

difficulties in SIMS analyses for biological applications such as posttranslational modifications. After deposition of AuNPs onto SAMs, the remaining surface can be easily modified with functionl groups to minimize nonspecific binding of proteins. In contrast to this SAMs/AuNPs assembly, bare gold would be susceptible to nonspecific adsorption by the reaction cascade of proteins. Last, AuNPs can be used for various surfaces including glass and silicon. When amine-modified glass and silicon were employed, similar results were obtained (Figure 7). In addition, the amount of peptides immobilized on AuNPs was considerably higher than that on SAMs (Table 2). It was reported that the surface densities of peptides immobilized on maleimide-terminated mixed SAMs[17] or by using a heterobifunctional cross-linker on amine SAMs[18] are 6.0×10^{12} and 1.5×10^{13} molecules·cm^{-2}, respectively. These amounts are a lower density than that of peptides adsorbed on SAMs/AuNPs. The three-dimensional structure of SAMs/AuNPs seems to provide more effective binding sites for peptides than SAMs by reducing the steric hindrance in peptide binding.

To demonstrate the utility of gold NE-SIMS in imaging a biomolecular surface, the P1 and P2 peptides were patterned on SAMs in the presence and absence of AuNPs using a microfluidic system of a BIAcore X instrument and imaged by TOF-SIMS. As

(15) Hagenhoff, B. In *ToF-SIMS: Surface analysis by mass spectrometry*; Vickerman, J. C., Briggs, D., Eds.; SurfaceSpectra: Manchester, 2001; pp 285−308.
(16) (a) Hong, M.-Y.; Yoon, H. C.; Kim, H.-S. *Langmuir* **2003**, *19*, 416−421. (b) Hong, M.-Y.; Lee, D.; Kim, H.-S. *Anal. Chem.* **2005**, *77*, 7326−7334.
(17) Houseman, B. T.; Huh, J. H.; Kron, S. J.; Mrksich, M. *Nat. Biotechnol.* **2002**. *20*, 270−274.
(18) Wegner, G. J.; Lee, H. J.; Corn, R. M. *Anal. Chem.* **2002**, *74*, 5161−5168.
(19) Cumberland, S. L.; Strouse, G. F. *Langmuir* **2002**, *18*, 269−276.
(20) Lahiri, J.; Isaacs, L.; Tien, J.; Whitesides, G. M. *Anal. Chem.* **1999**, *71*, 777−790.

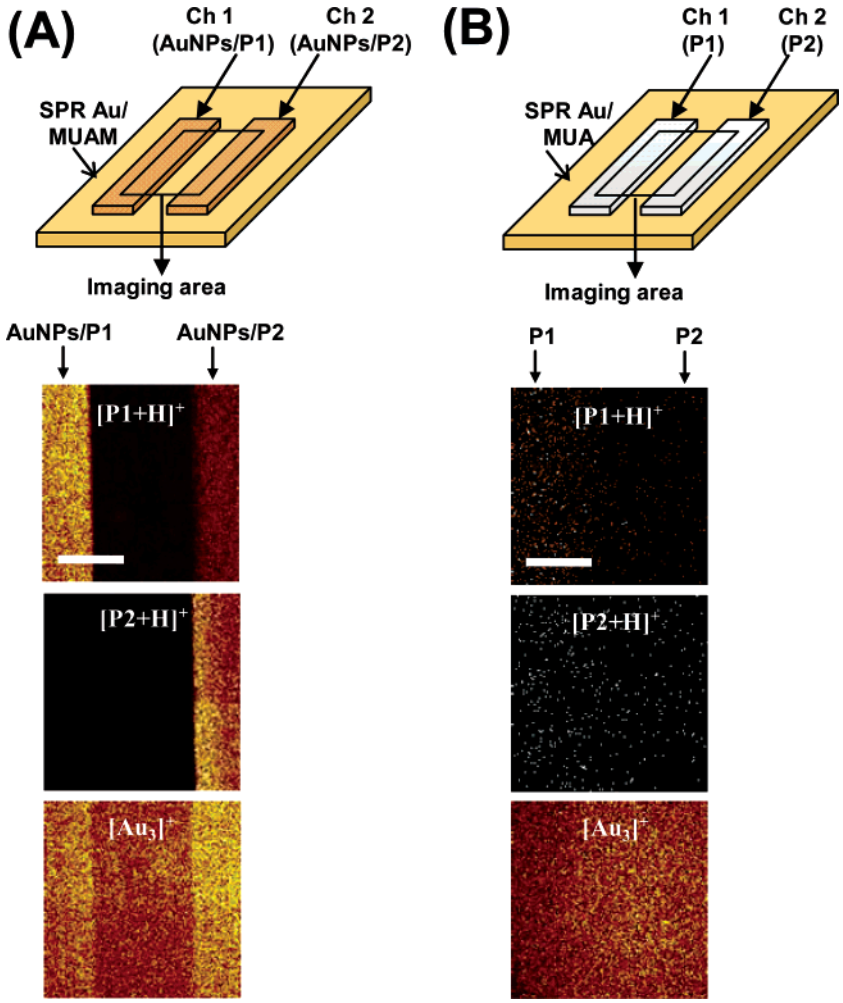

Figure 8. Positive TOF-SIMS images of $[P1 + H]^+$ at *m*/*z* 887, $[P2 + H]^+$ at *m*/*z* 967, and $[Au_3]^+$ at *m*/*z* 592 from peptides patterned on SAMs pretreated (A) with AuNPs and (B) without AuNPs. The lateral region at both sides (both arrows) represents a microfluidic pattern of different peptides (P1 and P2). The peptides were passed over the surface with a solution concentration of 50 μg·mL^{-1} for 30 min at a flow rate of 3 μL·min^{-1}. TOF-SIMS imaging was conducted using a Au_1^+ primary ion gun with an ion dose below 10^{13} ions·cm^{-2} at a sample area of 300 × 300 μm^2. The scale bar is 100 μm.

shown in Figure 8A, distinct chemical images of P1 and P2 peptides were observed at *m*/*z* 887 and 967, respectively, when patterned with AuNPs on SAMs. In contrast, no images were detected when the peptides were patterned directly onto SAMs without AuNPs (Figure 8B). The first image of Figure 8A shows a weak signal from the lateral region of AuNPs/P2, which corresponds to the loss of phosphate from the P2 peptide, viz. *m*/*z* $[(P2 - HPO_3) + H]^+$, although the authentic phosphopeptide (P2) used in our study was a 100% phosphorylated form. This weak signal, however, was negligible compared to the molecular ion of $[P2 + H]^+$, which showed an intense signal as shown in the second image of Figure 8A. In addition, the generation of secondary gold ions at *m*/*z* Au_3^+ by AuNPs is clearly demonstrated in the third image of Figure 8A, which indicates the formation of the AuNP monolayers in the MUAM SAMs. These results show that the use of NE-SIMS imaging is as an effective technique for identifying subtle chemical modifications (e.g., phosphorylation) in peptides patterned on a defined surface with an unambiguous assignment.

CONCLUSIONS

The emission of secondary ions of peptides immobilized on AuNPs was significantly enhanced in TOF-SIMS compared to those on SAMs. Distinct imaging of patterned peptides adsorbed on a submonolayer of AuNPs will expand the utility of gold NE-SIMS in the chip-based imaging analysis of biomolecules in a label-free manner.

ACKNOWLEDGMENT

This work was supported by the R&D Program of Fusion Strategies for Advanced Technologies of MOCIE, the Nano/Bio Science & Technology Program (M1053609000205N3609-00210) and the Nano Science & Technology Program (M10503000218-05M0300-21810) of MOST, and the Korea Health 21C R&D Project (0405-MN01-0604-0007) of MHW.

SUPPORTING INFORMATION AVAILABLE

Additional information as noted in text. This material is available free of charge via the Internet at http://pubs.acs.org.

Received for review August 21, 2005. Accepted January 11, 2006.

AC051500J